

AD 731414

KINETICS OF IRON AND ALUMINUM OXIDATION BY OXYGEN

First Annual Report

Arthur Fontijn and Shelby Kurzius

Sponsored by

Advanced Research Projects Agency, Dept. of Defense
under AO 1433, DNA, NWER Subtask ZL433

Contracting Agency
Defense Nuclear Agency
Contract No. DASA 01-70-C-0152

D D C
RECEIVED
OCT 26 1971
RECEIVED



AeroChem **Research Laboratories, Inc.**

SYBRON CORPORATION

Princeton, New Jersey

Approved for public release; distribution unlimited.

Reproduced by
**NATIONAL TECHNICAL
INFORMATION SERVICE**
Springfield, Va. 22151

**MISSING PAGE
NUMBERS ARE BLANK
AND WERE NOT
FILMED**

DOCUMENT CONTROL DATA - R & D

(Security classification of title, body of abstract and indexing information must be entered when the overall report is classified)

1. ORIGINATING ACTIVITY (Corporate author)		2a. REPORT SECURITY CLASSIFICATION	
AeroChem Research Laboratories, Inc. Sybron Corporation Princeton, N.J. 08540		UNCLASSIFIED	
3. REPORT TITLE		2b. GROUP	
Kinetics of Iron and Aluminum Oxidation by Oxygen			
4. DESCRIPTIVE NOTES (Type of report and inclusive dates)			
First annual report, 1 June 1970 to 31 May 1971			
5. AUTHOR(S) (First name, middle initial, last name)			
Arthur Fontijn and Shelby C. Kurzius			
6. REPORT DATE	7a. TOTAL NO. OF PAGES	7b. NO. OF REFS	
July 1971	30	17	
8a. CONTRACT OR GRANT NO.	9a. ORIGINATOR'S REPORT NUMBER(S)		
DASA 01-70-C-0152	AeroChem TP-260		
6. PROJECT NO. ARPA Order 1433	9b. OTHER REPORT NO(S) (Any other numbers that may be assigned this report)		
c. Program Code: OE50	DNA 2735 I		
d.			
10. DISTRIBUTION STATEMENT			
Approved for public release; distribution unlimited.			
11. SUPPLEMENTARY NOTES		12. SPONSORING MILITARY ACTIVITY	
Contracting Officer's Representative: Dr. Charles A. Blank, STRA Defense Nuclear Agency		Advanced Research Projects Agency 1400 Wilson Blvd. Arlington, Va. 22209	
13. ABSTRACT			
<p>Because of the need for quantitative information on gaseous metal atom oxidation kinetics, an experimental research program has been initiated to determine the mechanism and rate coefficients of the homogeneous reactions of free Fe and Al atoms with O_2^1. The apparatus used is a cylindrical fast-flow reactor, adapted for the study of the kinetics of refractory gaseous species at temperatures up to 1900 K.</p> <p>The Fe/O_2 reaction at 1600 K has been investigated in N_2/O_2 flows by observing the rate of decay of Fe-atom concentrations, measured in absorption, at pressures from 15 to 60 Torr. The gas phase reaction has been determined to be $Fe + O_2 \rightarrow FeO + O$, with a rate coefficient $k_2 = 4 \times 10^{-13}$ ml molecule⁻¹ sec⁻¹. This result is estimated to be accurate to within a factor of about 2. Evidence for heterogeneous oxidation of Fe in the presence of O_2 has also been obtained; the lower limit for the probability of Fe oxidation per collision with the reactor wall, γ, is found to be on the order of 1×10^{-1}. <i>1/10.7</i></p> <p>Exploitation and extension of the technique developed to determine the temperature dependence of k_2 and to obtain similar information for other reaction systems of interest will lead to data required for relevant DoD investigations not readily obtainable by other techniques.</p>			

*yields**k₂ = 4 x 10⁻¹³ ml/molecule/sec*

14 KEY WORDS	LINK A		LINK B		LINK C	
	ROLE	WT	ROLE	WT	ROLE	WT
Oxidation kinetics Fe vapor Metal oxides High temperature flow reactor						

July 1971

KINETICS OF IRON AND ALUMINUM OXIDATION
BY OXYGEN

First Annual Report

Arthur Fontijn and Shelby C. Kurzius

Sponsored by

Advanced Research Projects Agency, Dept. of Defense
under AO 1433, DNA, NWER Subtask ZL433

Contracting Agency
Defense Nuclear Agency
Contract No. DASA 01-70-C-0152

Contractor: AeroChem Research Laboratories, Inc., Princeton, N.J. 08540
Date of Contract: 12 June 1970
Amount of Contract: \$54,995
Contract Expiration Date: 31 August 1971
Contracting Officer's Representative: Dr. Charles A. Blank, STRA
Principal Investigator: Dr. Arthur Fontijn
Phone: (609) 921-7070



AeroChem **Research Laboratories, Inc.**

SYBRON CORPORATION

Princeton, New Jersey

Approved for public release; distribution unlimited.

SUMMARY

Because of the need for quantitative information on gaseous metal atom oxidation kinetics, an experimental research program has been initiated to determine the mechanism and rate coefficients of the homogeneous reactions of free Fe and Al atoms with O₂. The apparatus used is a cylindrical fast-flow reactor, adapted for the study of the kinetics of refractory gaseous species at temperatures up to 1900 K.

The Fe/O₂ reaction at 1600 K has been investigated in N₂/O₂ flows by observing the rate of decay of Fe-atom concentrations, measured in absorption, at pressures from 15 to 60 Torr. The gas phase reaction has been determined to be $\text{Fe} + \text{O}_2 \rightarrow \text{FeO} + \text{O}$, with a rate coefficient $k_2 = 4 \times 10^{-13} \text{ ml molecule}^{-1} \text{ sec}^{-1}$. This result is estimated to be accurate to within a factor of about 2. Evidence for heterogeneous oxidation of Fe in the presence of O₂ has also been obtained; the lower limit for the probability of Fe oxidation per collision with the reactor wall, γ , is found to be on the order of 1×10^{-1} .

Exploitation and extension of the technique developed to determine the temperature dependence of k_2 and to obtain similar information for other reaction systems of interest will lead to data required for relevant DoD investigations not readily obtainable by other techniques.

FOREWORD AND ACKNOWLEDGMENT

This is the first annual technical report on contract DASA 01-70-C-0152, "Kinetics of Atomic Fe and Al Oxidation by O₂," covering the period 1 June 1970 to 31 May 1971. The material covered herein supersedes that covered in the semi-annual report, AeroChem TN-145, issued in December 1970.

We thank James J. Houghton for his strong support in performing the experiments and Dr. John A. Emerson for his involvement with the preliminary work. We have benefited from many discussions with several members of the AeroChem staff, particularly with Dr. Robert K. Gould.

TABLE OF CONTENTS

	<u>Page</u>
SUMMARY	iii
FOREWORD AND ACKNOWLEDGMENT	v
LIST OF FIGURES	vii
I. INTRODUCTION	1
II. APPARATUS	1
A. General Description	1
B. Vacuum Furnace and Flow Reactor	2
C. Temperature Control and Measurement	3
D. Metal Atom and O ₂ Introduction Systems	4
1. Fe Introduction	4
2. Al Introduction	5
3. O ₂ Introduction	5
E. Optical System	5
III. EXPERIMENTAL	6
IV. DATA AND INTERPRETATION	9
V. DISCUSSION	12
VI. REFERENCES	13
TABLE I RUN RESULTS: Fe/O ₂ KINETICS	11

LIST OF FIGURES

<u>Figure</u>		<u>Page</u>
1	SCHEMATIC OF APPARATUS	15
2	FRONT VIEW OF REACTOR	16
3	REAR VIEW OF REACTOR	17
4	VACUUM FURNACE AND FLOW REACTOR	18
5	OPTICAL CONFIGURATION FOR RELATIVE METAL ATOM CONCENTRATION MEASUREMENTS	19
6	[Fe] AND REACTION TEMPERATURE PROFILE	20
7	[Fe] PROFILE	21
8	Fe/O ₂ REACTION RATE COEFFICIENT AT 15 TORR	22
9	Fe/O ₂ REACTION RATE COEFFICIENT AT 30 TORR	23
10	Fe/O ₂ REACTION RATE COEFFICIENT AT 60 TORR	24

I. INTRODUCTION

The goal of the present work is to measure rate coefficients for the reactions of gaseous Fe and Al with O_2 required for various Department of Defense applications.

The measurements are made with a heated cylindrical fast-flow reactor apparatus suitable for study of the kinetics of gaseous species at temperatures up to 1900 K. Rate coefficients are obtained from the observed variations in the relative metal atom concentration (measured in absorption) as a function of reaction time, O_2 concentration, and total pressure. The flow reactor is a high purity alumina cylindrical tube situated inside a vacuum furnace. The reactor and vacuum jacket have ports for optical observations. The metal is vaporized and entrained in an inert carrier gas stream. The O_2 is introduced into this gas stream at concentrations several orders of magnitude larger than that of the metal atoms. The basic measurement of the relative metal atom concentration as a function of reaction time is made via optical absorption of the requisite metal atom radiation emitted by a hollow-cathode lamp.

Although the general features of the apparatus and technique developed have been described elsewhere,¹ extensive modifications and preliminary experiments have been necessary to successfully adapt the apparatus to the study of refractory metal vapor oxidation kinetics, and the apparatus as it is now constituted is therefore described in Section II of this report. Experimental details are given in Section III. The results of the experiments, which so far have been restricted to the Fe/ O_2 reaction at 1600 K, are presented in Section IV and the inferred rate coefficient is discussed in Section V. Rate measurements at other temperatures, and for the analogous Al reaction, are to be made in the second year of this study.

II. APPARATUS

A. General Description

A simplified drawing of the apparatus is shown in Fig. 1. The 2.5 cm i.d. reaction tube is contained inside a 25 cm i.d. vacuum chamber. An inert gas (N_2 or Ar) passes through the reaction tube and entrains metal vapor either from a resistively-heated basket containing the metal or from an internally resistively-heated sleeve of the metal to be vaporized. (The latter technique has been used in the Fe/ O_2 study.) O_2 is introduced from the down-

stream end of the apparatus through a nozzle located at the end of a movable tube. The reaction time is proportional to the distance from this nozzle to the observation port and is varied by changing the nozzle position; metal atom concentrations in the gas arriving at the observation port are measured optically in absorption. The vacuum furnace is continuously purged with the aid of a sweeper gas flow.

Figures 2 and 3 show photographs of the apparatus as seen from the hollow-cathode metal atom emission line source and monochromator detector sides, respectively. Figure 4 schematically shows some of the internal details of the vacuum furnace and reactor, and Fig. 5 is a sketch of the optical path and the apparatus used to measure relative metal atom concentrations.

B. Vacuum Furnace and Flow Reactor

The essential features are shown in Fig. 4. The vacuum chamber, A, is a 25.0 cm i.d. brass cylinder, 95.0 cm long, closed at both ends by demountable flanges B_1 and B_2 . The 3.2 cm o.d., 2.5 cm i.d. flow reactor, C, is made of McDanel 998 alumina tubing (99.8% Al_2O_3). The reaction tube does not extend all the way to the downstream end of the jacket, thus making allowance for thermal expansion. An asbestos fiber collar, W, provides a flexible--but pervious--seal to induce the sweeper gas to flow through the observation ports, thereby retarding the leak of metal vapors from the flow reactor at these ports. The muffle (with three contiguous heating zones) D is composed of a grooved (with 0.8 cm pitch) 5.1 cm o.d., 4.5 cm i.d., 82 cm long McDanel 998 alumina core, wound with 0.127 cm diam Pt-40% Rh resistance wire. The two end zones and the central zone are each wired separately to maintain a uniform temperature over the 30 cm portion of reaction tube in which our measurements are made. The windings are coated with a layer of alumina cement and are each shielded by a 25 cm long, 6.0 cm o.d., 5.4 cm i.d. McDanel 998 alumina tube. The core is held in place by two stainless steel disks E_1 and E_2 (20 cm diam), which are fastened together by the rods Q_2 . These disks have grooves into which fit the core and three cylindrical radiation shields, F. The innermost--and hottest--shield is a 75 cm long, 11.4 cm o.d., 10.5 cm i.d. length of McDanel AV 30 alumina tubing (96% alumina). Molybdenum sheet (0.05 cm thick) is used for the two outer shields. The entire muffle assembly is supported by rods Q_1 connecting the top disk E_1 to the end plate B_1 of the vacuum housing A. By means of a hoist on the ceiling the whole furnace can be removed for inspection or repair. The entire vacuum chamber is surrounded by coiled copper tubing, G, through which cooling water is flowed at a constant rate.

The optical path for the measurement of the relative Fe-atom concentration by light absorption is provided by two 2.5 cm diam quartz windows in the vacuum jacket, which are aligned with 2.5 cm diam holes in the radiation shields and the muffle and the 1.2 cm diam open ports of the reaction tube. A

bottom flange seals the reaction tube to the vacuum jacket base flange B₂ via an O-ring seal I. Silver-brazed to the bottom flange is a stainless steel cross tube J, which provides the inlet K for the inert gas stream and connections to the 3.2 cm i.d. ball valve U and manometers M. The 1.9 cm o.d. alumina support tube L for the resistively heated vaporizer P can readily be withdrawn through the ball valve, thus permitting closure of the valve and complete isolation of the vaporizer from the reactor. This recently incorporated valve greatly facilitates making repairs to and replenishing the vaporizer without otherwise altering furnace conditions.

The inlets N make it possible to continuously sweep the vacuum jacket with a flow of gas. As an additional precaution, a small portion of the sweeper gas flow is admitted directly over the inside of the jacket windows. To overcome irreversible signal degradation during the experiments due to fogging of the windows,* the reactor observation ports are operated without windows.

C. Temperature Control and Measurement

The power supplies for each of the three heating zones are independent and manually controlled.† Each supply consists of a step-down transformer, a solid-state rectifier, a rheostat and a current meter. A 0.05 cm diam Pt vs. Pt-10% Rh thermocouple is situated on the outside of the reactor in the center of each heating zone. To permit taking a rapid approximate scan of the reactor temperature profile, two additional thermocouples are situated on the outside of the reactor, with the result that reactor external temperature measurements can be made 2, 7, 12, 24 and 42 cm upstream of the observation port. The leads for these thermocouples are fed through the side of the vacuum jacket via the vacuum feed-through R. The maximum power consumption is approximately 9.3 kVA, with 45 amperes and 70 V per zone. The actual reaction temperature is measured by a 0.025 cm diam Pt vs Pt-10% Rh thermocouple adjacent to the tip of the O₂ inlet with leads fed through the stainless steel tube S (Fig. 4 and Section II.D.3).

To protect the furnace against accidental burn-out, sensing devices have been interlocked with its power supply so that, in the event of a pressure leak, a power failure, or a cooling water supply interruption, the heating

* Encountered in this work in attempted preliminary Fe/O₂ rate studies in which initially transparent sapphire windows were used to seal the reactor.

† Automatic digital temperature controllers are also available. However, in practice we have found it more convenient and more reliable to manually control the muffle currents.

elements will be automatically turned off. The interlock system must be reset manually. These precautions are highly desirable for the periods of unattended operation of the furnace, which is continuously kept at high temperatures.

D. Metal Atom and O₂ Introduction Systems

To introduce metal atoms of low volatility elements, such as Fe and Al, two methods appeared suitable a priori: (i) use of a resistively-heated metal source placed inside the reaction tube, or (ii) introduction of volatile organometallic compounds such as, e.g., Fe(CO)₅ or Al(CH₃)₃, which would decompose upon introduction to the reactor. Of these methods, the former seemed straightforward and simpler and was therefore chosen. The variation of the technique used for Fe vapor studies differs from that planned for Al-vapor studies; both are described below.

1. Fe Introduction

The present Fe/O₂ rate study has been performed at a reaction temperature of 1600 ± 30 K. At this temperature the equilibrium saturation vapor pressure of Fe is ≈ 10⁻³ Torr,^{3,4} corresponding to [Fe] ≈ 6 × 10¹² ml⁻¹, which is sufficient to give ≈ 90% absorption of the Fe 3720 Å line (Section III). Since 1600 K is considerably below the melting point of Fe (1809 K)^{3,4} it is not necessary to heat the Fe to its melting point to obtain an adequate gas phase Fe atom concentration. The Fe is therefore evaporated simply by using an inverted pure Fe beaker, 4 cm long, 1.2 cm o.d., 1.0 cm i.d. This beaker is resistively heated from within, using 0.08 cm diam tungsten wire wound over a 0.5 cm o.d., 0.2 cm i.d. alumina tube. The tungsten-wound ceramic fits snugly into an alumina liner (0.95 cm o.d., 0.7 cm i.d.) placed into the Fe beaker. This assembly is placed directly inside the reaction tube on top of the open-ended 1.9 cm o.d., 1.6 cm i.d. alumina support tube L, movable in the axial direction.

Power for the beaker assembly is provided by a stable power supply (Kepco PR 40-50M) through 0.25 cm diam Mo rods containing 1 cm long, 0.09 cm diam holes into which the W heating wire ends are fitted. A Pt vs. Pt-10% Rh thermocouple is embedded in alumina cement in a notch cut in the center of the Fe beaker for this purpose. This thermocouple is used for manual control of the Fe-beaker temperature.

In normal operation with a new beaker, a stable Fe-atom flow is obtained with a heating current of ≈ 10 amp. Beaker temperatures approaching 1800 K are, however, found to be required and within a few days the beakers begin to sag and lose their structural integrity, requiring currents approaching ≈ 20 amp to give the required Fe-atom flows. The useful lifetime of the beakers is on the order of 3 to 4 days of experiments. An appreciable build-up of

condensed metal is observed at the (relatively cool) closed end of the beaker, probably explaining why a temperature approaching 1800 K is necessary to obtain an adequate Fe-atom flow downstream of the vaporizer.

2. Al Introduction

Al melts at 933 K, while an equilibrium saturation vapor pressure of $\approx 10^{-3}$ Torr (which we estimate to be required) is first achieved at 1370 K.^{3,4} Thus it is necessary to contain Al as a liquid in the vaporizer. To accomplish this the metal is placed inside a 3.8 cm long, 1.3 cm i.d. crucible heated by 0.05 cm diam W wire which surrounds and supports it.* This assembly is covered by alumina cement and is placed on the alumina support tube L as discussed above.

3. O₂ Introduction

A movable ceramic nozzle is employed for this purpose. The O₂ flows through a 0.16 cm i.d. alumina tube extended from a mating stainless steel tube, S, (Fig. 4). This tube is offset 0.6 cm laterally from the center axis of the reaction tube, so that the alumina tube does not block the radiation used in measuring the relative metal atom concentration, and can be moved axially through sliding O-ring seals, I, to vary the reaction time. An alumina-coated 0.3 cm diam Pt disk, suspended (by alumina-coated Pt wires) ≈ 0.2 cm below the open end of the O₂ inlet is used to distribute the O₂ as uniformly as possible over the reactor cross sectional area.

The O₂ nozzle can be moved from a position downstream from the reactor observation port to one 30 cm upstream from it.

E. Optical System

The optical system used in the measurement of relative Fe concentrations is shown in Fig. 5. A Westinghouse WL-22810A high spectral output Neon-filled hollow cathode Fe lamp, A, powered by a stabilized ($\pm 0.1\%$) current-regulated dc supply (Electronic Measurements C 636), is used as the light source. The light from this source is sent through a vibrating (140 Hz) slit

* This method has already been used successfully in our Na studies⁵ in the present apparatus and is similar to that used by Ferguson, Fehsenfeld, et al in their metal ion flow reactor studies.^{6,7} Alumina, carbon and boron nitride crucibles have been selected for their compatibility⁸ with the metals of interest in the present studies.

chopper B, and then passes through the reactor. The condensing lens C focuses the radiation on the entrance slit of the monochromator D. The latter is a Jarrell-Ash 82000 Ebert-mounting 0.5 meter grating instrument equipped either with an HTV-R212 photomultiplier tube for observation of the Fe I 3720 Å absorption line, or with an HTV-R166 solar blind tube for observation of the Fe I 2483 Å absorption line. The photomultiplier output is measured with a PAR Model HR-8 phase-sensitive lock-in amplifier.

III. EXPERIMENTAL

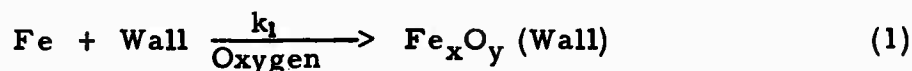
Routine⁹ gas handling procedures are employed. Linde high purity dry N₂, from a liquid N₂ container, is used for both the reactor bath gas and the sweeper gas, Fig. 1. The O₂ used is Linde U.S.P. All gases are passed through columns containing an activated alumina drying agent before being metered. Linde high purity dry Ar was used as the bath gas in a few experiments in which it was established that N₂ does not react with Fe at a measurable rate.

The pressure is continuously indicated by an Alphatron pressure gauge, and is measured absolutely by one of three manometers connected in parallel to a side tube of the flow reactor. These manometers are: i) for the 0.5 to 4 Torr range, a precision U-tube dibutylphthalate oil manometer⁹; ii) for the 4 to 50 Torr range a precision U-tube mercury manometer; iii) for higher pressures a conventional mercury manometer. Pressure at a given flow rate is controlled by a throttling valve in the line to the 130 CFM vacuum pump, and pressure taps upstream and downstream of the reactor are provided to check that the pressure drop across the reactor is not significant.

To effectively prevent the reaction gases from entering the vacuum jacket through the reaction tube ports, a sweeper gas volume flow rate of about one fourth that of the reaction tube flow rate is passed through the furnace. The flow of sweeper gas into the reactor at the observation ports does not, however, interfere with our ability to make meaningful metal atom oxidation rate measurements, since these measurements are based on the change in reactant concentration as a function of reaction time when the O₂ nozzle is moved between points well upstream from the observation point. The validity of operating in this manner has been demonstrated by other workers^{10,11} concerned about having the measurement station at a much lower temperature than that of the reaction measured. We have, further, found it useful to add ≈ 1% O₂ to the sweeper gas to chemically scavenge residual vapors in the furnace. This slightly oxidizing atmosphere is also beneficial for the Pt/40% Rh muffle heating elements, protecting them from chemical attack by metal vapors.¹²

The range of experimental parameters explored so far is: $P = 3$ to 60 Torr; $[O_2] = 1 \times 10^{12}$ to 1×10^{16} ml⁻¹; bath gas = N₂; $\bar{T} = 1600 \pm 30$ K; mean gas velocity, $\bar{v} = 20$ to 50 msec⁻¹.

The 15 to 60 Torr range was found to be suitable for the study of the homogeneous gas phase oxidation reaction.* The first experiments were performed at 3 Torr. At this pressure a rapid reaction is observed when O₂ is introduced. This reaction is found to be of zero order in $[O_2]$ over the range 1×10^{12} to 2×10^{13} ml⁻¹, strongly indicative of a wall reaction, i. e.,



From these experiments the lower limit for the oxidation probability[†] per Fe atom collision with the wall, γ_{1600K} , is inferred to be on the order of 1×10^{-1} . To definitively determine this number, work at appreciably lower pressures would be required to remove diffusional transport limitations complicating the measurement of γ at 3 Torr. However, since the goal of the present experiments is to study the homogeneous reaction it was clearly necessary to work at pressures well above 3 Torr, to suppress the contribution of the heterogeneous reaction.

* In this range no pressure drop (i. e., $\Delta p < 0.2$ Torr) along the length of the reactor could be observed.

† Interpretation of the $[Fe]$ -decay profiles at 3 Torr according to the simple plug flow or parabolic flow analyses (Section IV) yields a value of $1.7 \pm 0.5 \times 10^3$ sec⁻¹, or $2.7 \pm 0.8 \times 10^3$ sec⁻¹, for k_1 , respectively. In the absence of diffusional limitations simple kinetic theory yields (see e. g. Ref. 13) $k_1 = (v_{Fe}/4)\gamma(\text{Surface Area/Volume})$, where v_{Fe} is the mean thermal velocity of Fe atoms. Using this relation, we calculate a value for γ of 0.54×10^{-1} or 0.88×10^{-1} from the data, corresponding to the plug flow or parabolic flow interpretation, respectively. Diffusional limitations are, however, non-negligible, even at 3 Torr; thus, for pure diffusion control, $k_1 = (23.2/d^2)D_{Fe}$ for plug flow⁷ and $k_1 = (14.6/d^2)D_{Fe}$ for parabolic flow,⁷ where D_{Fe} is the diffusivity of Fe atoms. We estimate, following the procedures of Ref. 14, $D_{Fe} \approx 0.76 \times 10^3$ cm²sec⁻¹ at 3 Torr and 1600 K, which yields $\approx 2.8 \times 10^3$ sec⁻¹ and $\approx 1.7 \times 10^3$ sec⁻¹ for k_1 , diffusion-controlled, for plug and parabolic flow, respectively. Since the observed values of k_1 are so close to the diffusion-limited values, the value of γ obtained has to be considered a lower limit.

Temperature at a given station in the reactor remained constant to within ± 5 K during experiments. However, depending to some extent upon flow conditions, significantly larger temperature variations were observed along the reaction tube axis. A particularly strong drop occurs close to the observation port, which acts effectively as a heat sink in a radiant enclosure. In addition to flow disturbances near the ports (see above), this was a reason to reject the data obtained close to the ports. An appreciation of the relatively shallow temperature gradients observed over the useful data range may be obtained from the centerline thermocouple readings shown in Fig. 6. \bar{T} has been taken from the average of these readings over the linear region of the reaction zone in plots such as in Fig. 6. In some experiments, as in those corresponding to Fig. 7, the centerline thermocouple was not functioning. For these runs \bar{T} has been taken as 20 ± 10 K less than the mean temperature reading of the thermocouples mounted on the outside of the reactor at 7 cm and 12 cm downstream of the reactor port. This correlation has been observed to hold in the experiments for which both sets of thermocouple measurements were available.

To ascertain that the optical absorption measurements of the relative Fe concentration were not influenced by other factors (e. g. the presence of nucleated products) the intensity of the Ne 5852 Å line, emitted by the hollow-cathode lamp, was routinely monitored. No attenuation of this line could be observed.

Knowledge of the absolute values of $[\text{Fe}]$ are not needed in the analysis of the experiments; however the data interpretation (see Section IV) implicitly requires $[\text{O}_2] \gg [\text{Fe}]$. $[\text{Fe}]$ can be estimated via the Lambert-Beer law:

$$[\text{Fe}] = \text{Constant} \times \ln(I_0/I)_\lambda \quad (\text{A})$$

in which the quantity I_0/I corresponds to the intensity ratio of the monitored beam of radiation of wavelength λ incident on the detector in the absence (I_0) and presence (I) of Fe. The value of the constant in Eq. (A) for the Fe 3720 Å line has recently been estimated by Linevsky,^{15,16} using a narrow-line width source, as 4.2×10^{11} particles ml^{-1} for a 15 cm path at 1500 K. For our 2.5 cm path this number becomes 2.5×10^{12} particles ml^{-1} . The fractional absorption $(I_0-I)/I_0$ observed in the present experiments varied from as high as $\approx 90\%$ at the upstream end of the reaction zone to as low as $\approx 1\%$ at the detection threshold, corresponding to $6 \times 10^{12} \text{ ml}^{-1} > [\text{Fe}] > 3 \times 10^{10} \text{ ml}^{-1}$. Since the constant in Eq. (A) is affected somewhat by pressure broadening^{15,16} these numbers probably are somewhat too high. The $[\text{O}_2]$ used in the determination of the homogeneous rate coefficient was in the range 1×10^{14} to $1 \times 10^{16} \text{ ml}^{-1}$, thus the condition $[\text{O}_2] \gg [\text{Fe}]$ was satisfied.

IV. DATA AND INTERPRETATION

The methods for determining rate coefficients from cylindrical fast-flow reactor experiments are well established (see e. g. Refs. 7 and 13). In the present work the rate coefficients for the Fe/O₂ reaction have been measured from the variation in relative Fe-atom concentration* as a function of reaction time, bulk O₂ concentration, and total pressure. Results of representative experiments are shown in Figs. 6 and 7. In these figures, the measured quantity $\ln(I_0/I)$ has been plotted on semi-logarithmic co-ordinates versus the distance of the O₂ inlet upstream of the observation port centerline. Since the relative Fe concentration is proportional to $\ln(I_0/I)$ (cf. Eq. (A)), plots such as Figs. 6 and 7 are therefore semi-logarithmic plots of relative Fe-atom concentration versus reaction time (a function of the distance between the O₂ inlet and the port) at constant values of [M] and [O₂]. Kinetic analysis of such data is relatively straightforward for simple plug flow (i. e., for flow with a flat velocity profile) with non-catalytic walls,^{7,13} or for simple laminar flow (i. e., for flow with a parabolic velocity profile) with active catalytic walls.⁷ As shown by Ferguson et al.,⁷ sophisticated numerical calculational models which incorporate such departures from ideal behavior as the effects of reactant inlets on the reacting species distribution within the reactor, pressure gradients, axial and radial diffusion, and slip velocity, yield results which are intermediate between the extremes derived from the simple plug and parabolic flow models, which in themselves yield not greatly divergent results. Thus we have evaluated the experimental data in terms of each of these models, though the parabolic profile probably approximates our conditions more closely.

For pseudo-first order disappearance of Fe, $-d[\text{Fe}]/dt = k_{ps1} [\text{Fe}]$ i. e., $k_{ps1} = -d \ln[\text{Fe}]/dt$. From the local slope, $a = -d \ln[\text{Fe}]/dx$, of the data plots (see e. g. Figs. 6 and 7), the pseudo-first order rate coefficient k_{ps1} is obtained via the equation

$$k_{ps1} = \eta a \bar{v} (1 + a D_{\text{Fe}}/\bar{v}) \quad (\text{B})$$

In Eq. (B) η is a factor equal to 1 for plug flow and approximately equal to 1.6 (Ref. 7) for parabolic flow, \bar{v} is the mean bulk linear gas velocity, D_{Fe} is the diffusivity of Fe atoms, and $(1 + a D_{\text{Fe}}/\bar{v})$ is the correction factor[†] for the effect of axial diffusion.¹³

* Hereafter indicated by [Fe].

† This correction was found to yield less than a 10% change in rate coefficients for the conditions of Table 1.

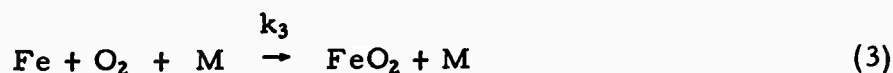
The rate coefficient k_{ps_1} incorporates the summation of heterogeneous and homogeneous contributions to the rate, i. e.,

$$k_{ps_1} = k_1 + k_2[O_2] + k_3[O_2][M] \quad (C)$$

where k_1 is the wall contribution and k_2 and k_3 correspond to the binary and ternary reactions of Fe with O_2 , i. e., to the reactions



and



A series of measurements of k_{ps_1} at constant temperature as a function of $[O_2]$ at various constant values of $[M]$ identifies the dominant homogeneous reaction and its rate coefficient. Results of three series of such measurements are shown in Figs. 8, 9 and 10,* which pertain respectively to experiments performed at 15, 30 and 60 Torr, with $\bar{T} = 1593, 1594$ and 1597 K. (\bar{T} for a series of experiments is taken as the average of the \bar{T} 's of the individual experiments comprising the series.)

The linearity of semi-logarithmic plots of $\ln(I_0/I)$, (i. e., $\ln[Fe]$), versus the reaction coordinate, as in Figs. 6 and 7 and of arithmetic plots of k_{ps_1} versus $[O_2]$, as in Figs. 8, 9 and 10 strongly indicates that the gas phase Fe/ O_2 reaction is first order in both $[Fe]$ and $[O_2]$. From the results, summarized in Table I, it is evident that the measured slopes of k_{ps_1} versus $[O_2]$ (i. e., $k_2 + k_3[M]$) do not increase with $[M]$, when $[M]$ is varied from 0.9×10^{17} to 5.4×10^{17} ml⁻¹. Thus $k_2 \gg k_3[M]$ under the conditions of the present experiments, i. e. the observed process is Reaction (2), for which the inferred rate coefficient is 4×10^{-13} ml molecule⁻¹ sec⁻¹. The non-zero extrapolated intercept of, e. g., Figs. 8, 9 and 10 is indicative of the parallel heterogeneous reaction path (Section III). The linearity of the observed plots and the relative constancy of the results also appears to rule out major influences of any other competing processes.

* The values of k_{ps_1} shown in Figs. 8, 9 and 10 correspond to the parabolic flow model.

Table I

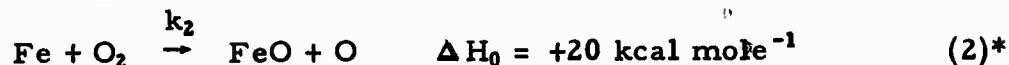
RUN RESULTS: Fe/O₂ KINETICS $(\lambda = 3720 \text{ \AA})$

<u>P</u> <u>(Torr)</u>	<u>v̄</u> <u>(m sec⁻¹)</u>	<u>[O₂]</u> <u>(10¹⁵ ml⁻¹)</u>	<u>[M]</u> <u>(10¹⁷ ml⁻¹)</u>	<u>T̄</u> <u>(K)</u>	<u>d k_{ps1}/d[O₂] = k₂ + k₃[M]</u> <u>(10⁻¹³ ml molecule⁻¹ sec⁻¹)</u>	
					<u>Plug Flow</u>	<u>Parabolic Flow</u>
15	49	0.1 to 6.8	0.91	1593 ± 20	3.9	6.4
30	24	0.9 to 10.3	1.8	1608 ± 20	2.8	4.6
30	24	0.2 to 5.2	1.8	1594 ± 20	2.5	4.0
30	24	0.2 to 5.3	1.8	1606 ± 20	2.4	3.8
60	24	0.2 to 7.0	3.6	1597 ± 20	2.2	3.6

Mean: 1600 ± 30
 $4(\bar{x} \pm 2) \times 10^{-13}$

V. DISCUSSION

The data collected in Table I lead to a value for the gas-phase rate coefficient of the reaction



of 4×10^{-13} ml molecule⁻¹ sec⁻¹ at 1600 K. The accuracy of this determination, taking into account possible systematic errors in reactant concentrations, etc., is probably to within a factor of 2. However, some additional experiments are desirable to further rule out the possibility of systematic error. Most important here would be the use of the Fe 2483 Å line in some experiments, thus changing both [Fe] and line profiles; a few preliminary experiments already made suggest that similar data will be obtained using the 2483 Å line. Also variation of \bar{v} at constant pressure appears desirable; here again preliminary data points suggest no strong dependence on this factor.

The next major step needed in this study is the experimental determination of the temperature dependence of k_2 . If, for the present, we assume the activation energy of the reaction to be approximately equal to the estimated endothermicity, then the above result corresponds to

$$k_2 = 2 \times 10^{-10} \exp(-20,000/RT) \quad (E)$$

This pre-exponential factor is within a factor of 2 to 3 of the collision frequency rate factor, which makes it unlikely that the activation energy can be appreciably greater than 20 kcal mole⁻¹, or that k_2 , 1600 K can be appreciably faster than measured here.

Two approximate limits on k_2 have been set by other workers. von Rosenberg and Wray¹⁷ found in shock tube work that at temperatures of 2400 K and greater, $k_2 \geq 5 \times 10^{-12}$. Equation (E) yields 3×10^{-12} at 2400 K in good agreement with von Rosenberg and Wray's limit. This also suggests that k_2 cannot be significantly lower than measured in the present work. Linevsky's flame studies¹⁶ yield the conclusion that k_2 , 1500 K $\geq 10^{-14}$, also consistent with the present result.

* ΔH_0 obtained from the JANNAF Thermochemical Tables.

VI. REFERENCES

1. Fontijn, A., "Kinetics of Homogeneous Reactions Between Free Metal Atoms and Hot Air Species -- Method and Apparatus," AeroChem TP-236, Final Report, March 1970.
2. Borucka, A. Z., "Design and Performance of an Electric Furnace for Precise Control of Temperature in the Range 700° - 1,300°C," Special Ceramics, Ed. P. Popper (Academic Press, New York, 1960), p. 265.
3. Honig, R. E. and Kramer, D. A., "Vapor Pressure Data for the Solid and Liquid Elements," RCA Review 30, 285 (1969).
4. Honig, R. E., "Vapor Pressure Data for the Elements," The Characterization of High-Temperature Vapors, ed. J. L. Margrave (J. Wiley, New York, 1967), Appendix A.
5. "Kinetics of Sodium and Potassium Reactions with High-Temperature Air Species," Sandia Contract 48-8290.
6. Ferguson, E. E. and Fehsenfeld, F. C., "Some Aspects of the Metal Ion Chemistry of the Earth's Atmosphere," J. Geophys. Res. 73, 6215 (1968).
7. Ferguson, E. E., Fehsenfeld, F. C., and Schmeltekopf, A. L., "Flowing Afterglow Measurements of Ion-Neutral Reactions," Advances in Atomic and Molecular Physics, Vol. 5, eds. D. R. Bates and I. Estermann (Academic Press, New York, 1969), Chap. 1.
8. Smith, J. M., "Selection of Materials," High-Temperature Materials and Technology, eds. I. E. Campbell and E. M. Sherwood (Wiley, New York, 1967), Chap. 5.
9. Fontijn, A., Miller, W. J. and Hogan, J. M., "Chemi-Ionization and Chemiluminescence in the Reaction of Atomic Oxygen with C₂H₂, C₂D₂, and C₂H₄," Tenth Symposium (International) on Combustion (The Combustion Institute, Pittsburgh, 1965), p. 545.
10. Westenberg, A. A. and de Haas, N., "Atom-Molecule Kinetics at High Temperature Using ESR Detection. Technique and Results for O + H₂, O + CH₄, and O + C₂H₆," J. Chem. Phys. 46, 490 (1967).
11. Clyne, M. A. A. and Thrush, B. A., "Rate of Elementary Processes in the Chain Reaction between Hydrogen and Oxygen. I. Reactions of Oxygen Atoms," Proc. Roy. Soc. (London) A275, 544 (1963).

12. Matthey Bishop, Inc., Technical Data Sheet PGM-1, September 1968.
13. Kaufman, F., "Reactions of Oxygen Atoms," Progress in Reaction Kinetics, Vol. 1, ed. G. Porter (Pergamon Press, New York, 1961), Chap. 1.
14. Reid, R.C. and Sherwood, T.K., The Properties of Gases and Liquids, Second Ed. (McGraw-Hill, New York, 1966).
15. Linevsky, M.J., "Study of Optical Energy Transfer Processes," General Electric Co., Valley Forge Space Center, Philadelphia, Pa., RADC-TR-69-87, February 1969
16. Linevsky, M.J., "Metal Oxide Studies," General Electric Co., Valley Forge Space Center, Philadelphia, Pa., RADC-TR-71-96, May 1971.
17. von Rosenberg, C.W. and Wray, K.L., "Metal Oxide Chemistry and Infrared Band Intensities," AVCO Everett Research Laboratory, Everett, Mass., AFCRL-70-0597, Final Report, October 1970.

70-136A

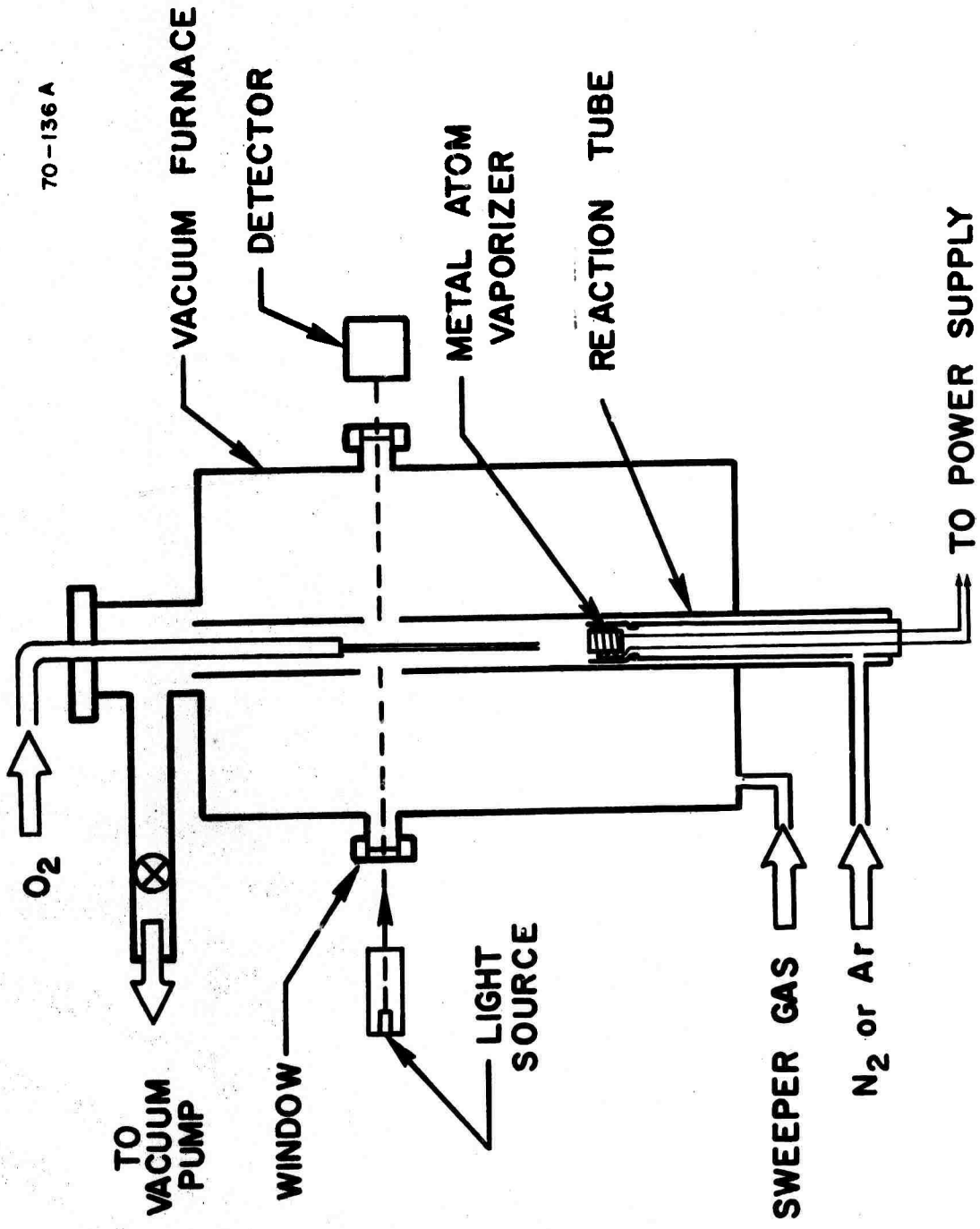


FIG. 1 SCHEMATIC OF APPARATUS

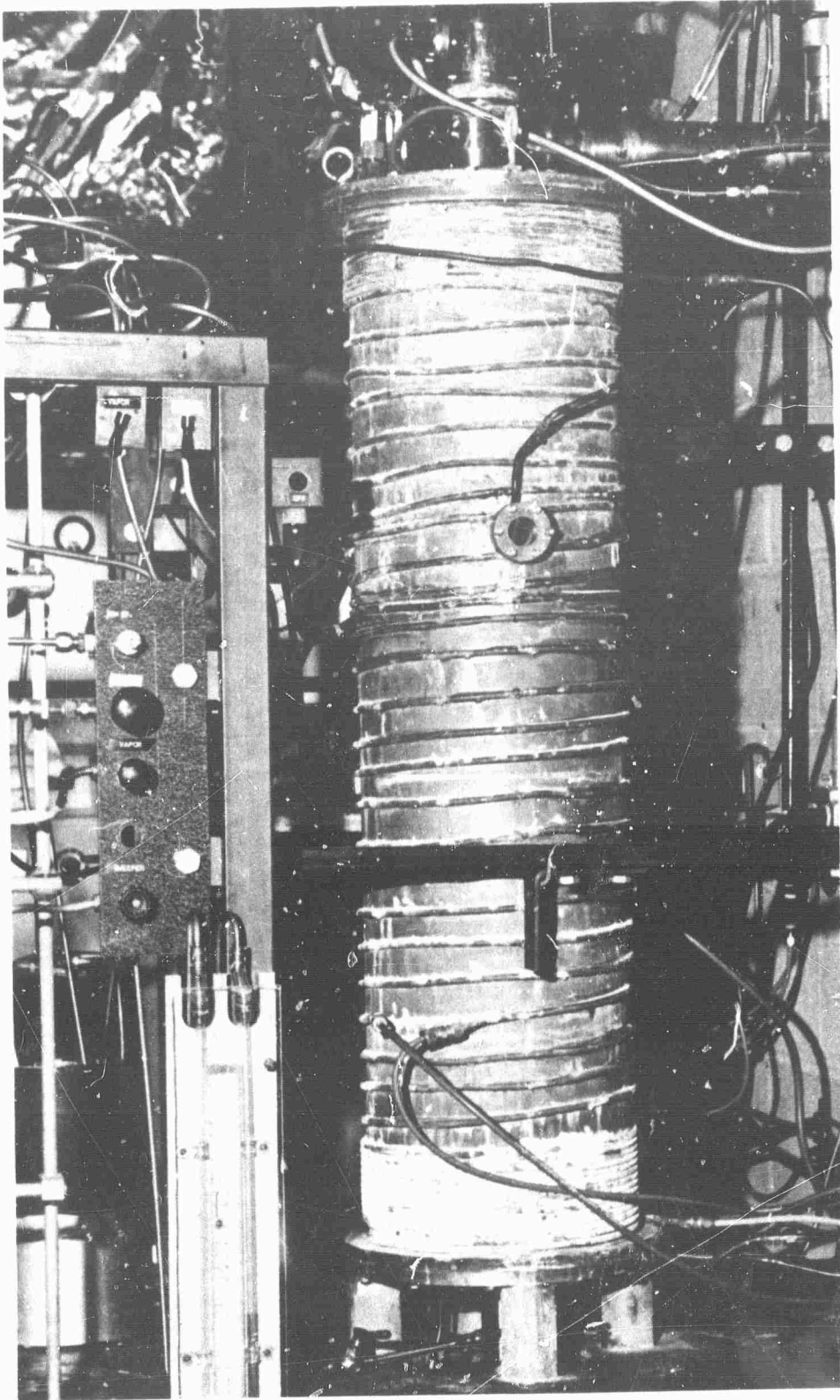


FIG. 2 FRONT VIEW OF REACTOR

The hollow cathode light source and light chopper, normally placed in front of the window, have been removed.

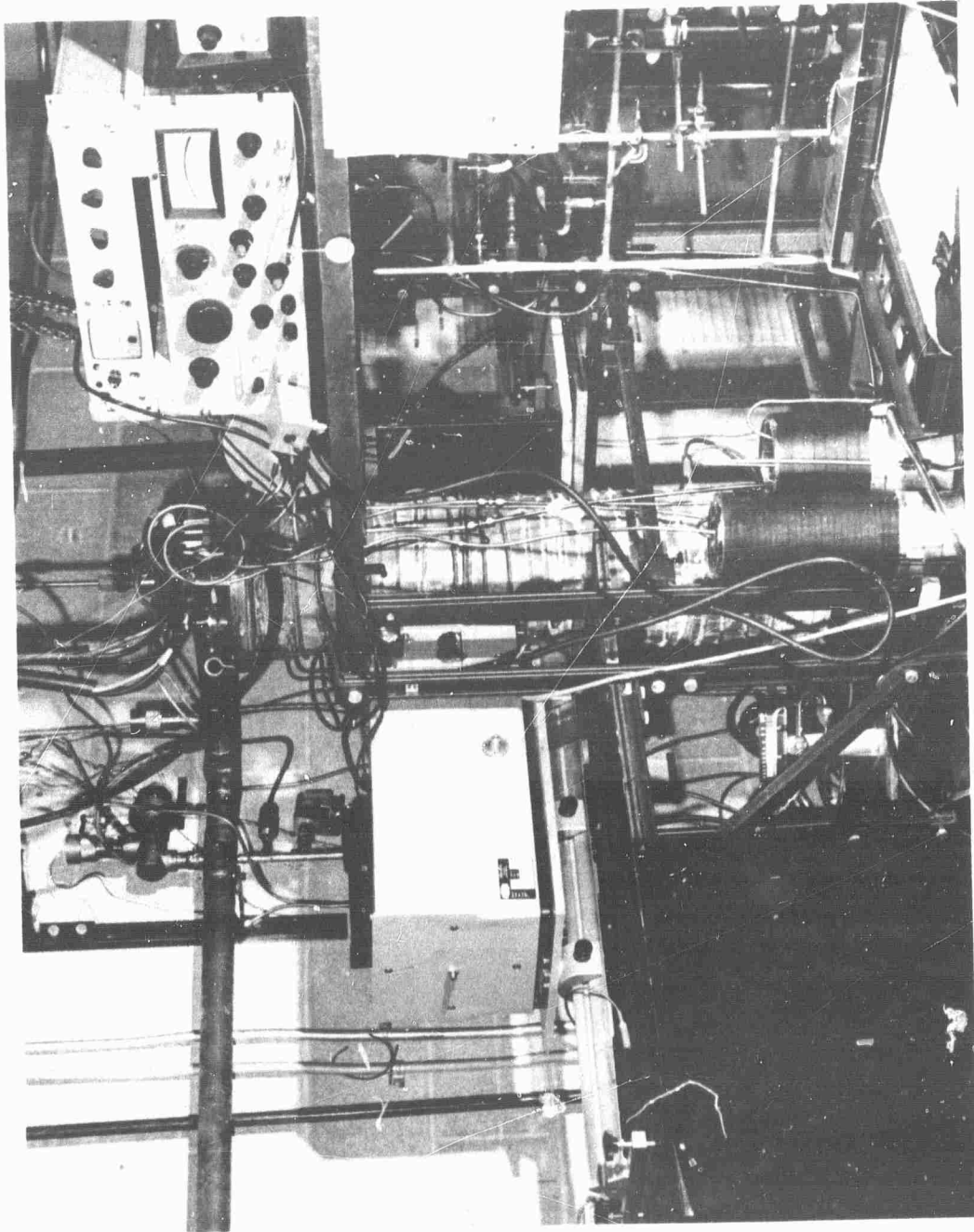


FIG. 3 REAR VIEW OF REACTOR

Also shown are the 0.5 meter monochromator, used to measure light absorption by the metal atoms, and the photomultiplier tube electronics.

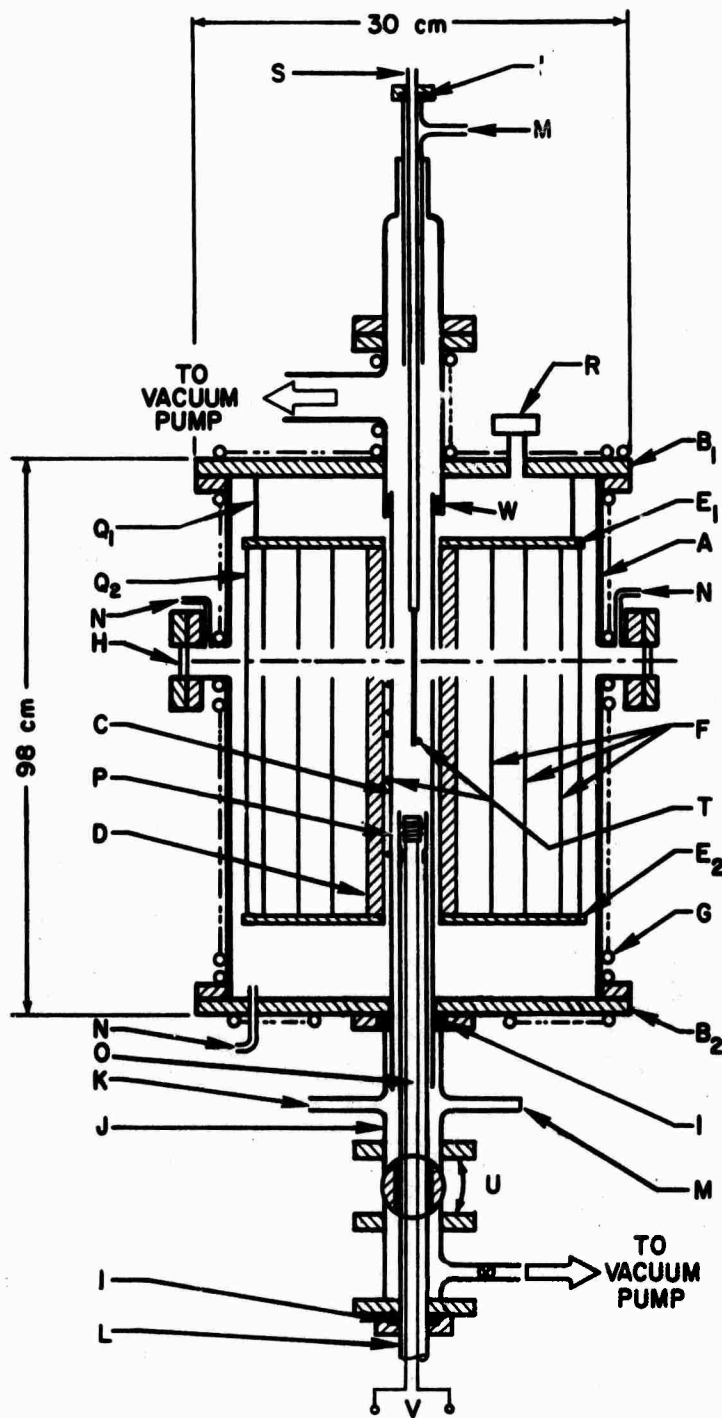


FIG. 4 VACUUM FURNACE AND FLOW REACTOR

A, vacuum jacket; B, flange; C, reaction tube; D, heating element (resistance wire and its connections not shown); E, supporting disk; F, radiation shield; G, cooling coil; H, window; I, O-ring seal; J, connecting cross; K, N_2 or Ar inlet; L, support tube for heated crucible assembly; M, manometer outlet; N, sweeper gas inlet; O, crucible power leads and thermocouple assembly; P, heated crucible; Q, support rod; R, vacuum feed-through for the thermocouples situated on the outside of the reactor; S, O_2 introduction system; T, thermocouple (6); U, ball valve; V, vaporizer power supply; W, asbestos fiber collar.

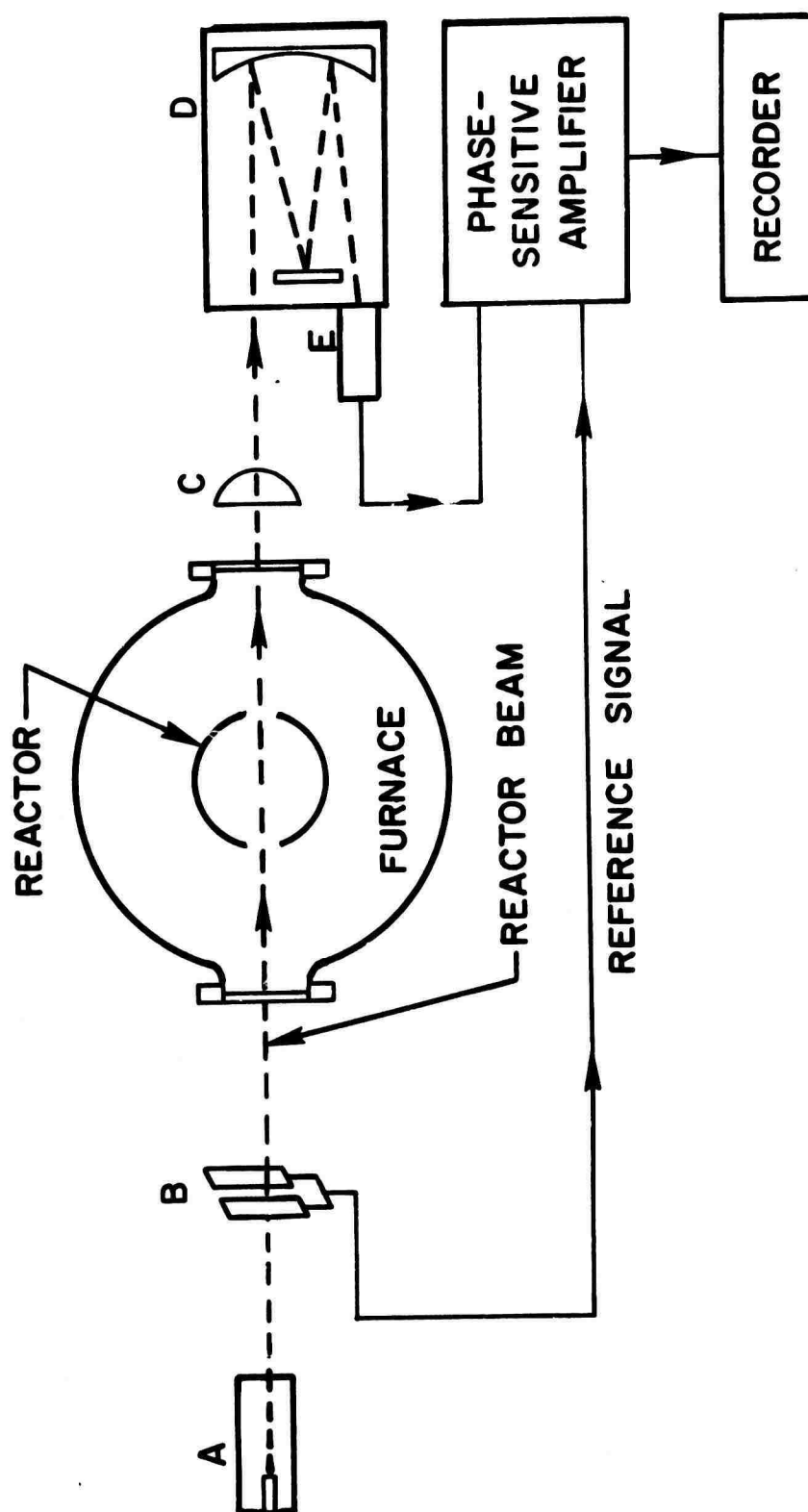
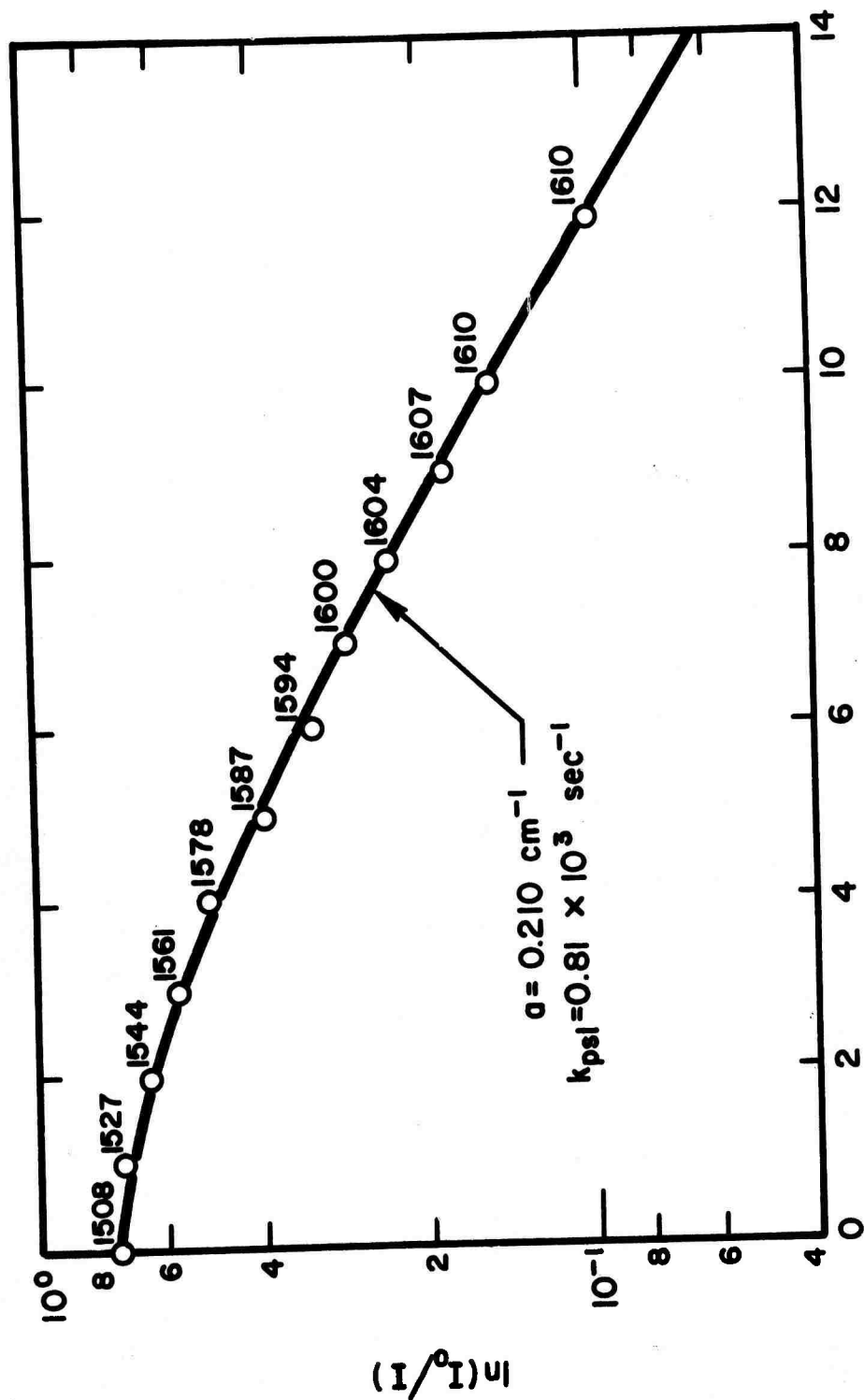


FIG. 5 OPTICAL CONFIGURATION FOR RELATIVE METAL ATOM CONCENTRATION MEASUREMENTS

A, hollow cathode lamp; B, chopper (vibrating slit); C, condensing lens; D, monochromator; E, photomultiplier tube.

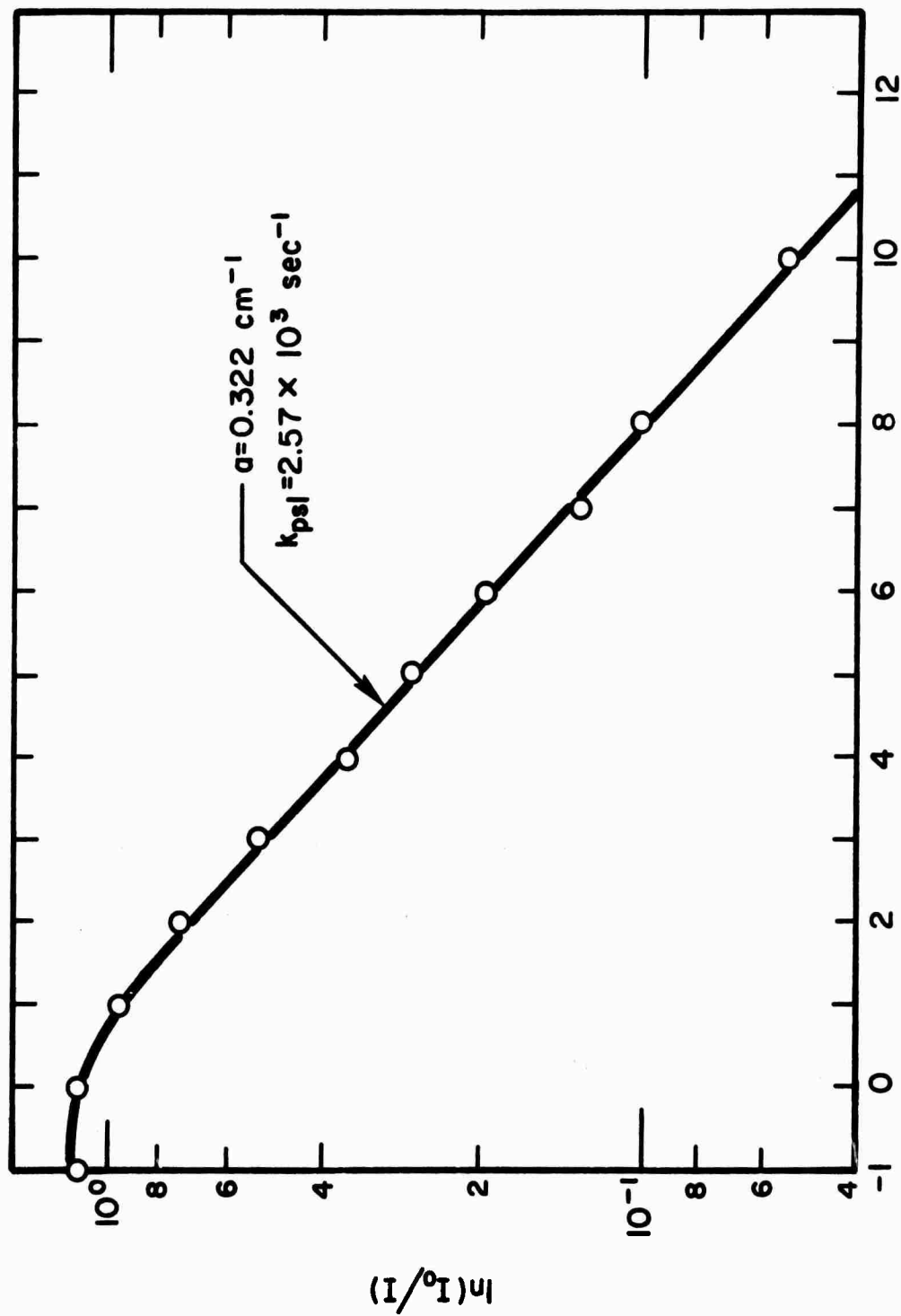


DISTANCE O₂ INLET TO PORT, cm

FIG. 6 [Fe] AND REACTION TEMPERATURE PROFILE

$$\begin{aligned}
 T &= 1605 \text{ K} \\
 v &= 23.9 \text{ m sec}^{-1} \\
 [\text{O}_2] &= 0.18 \times 10^{15} \text{ ml}^{-1} \\
 \lambda &= 3720 \text{ \AA} \\
 P &= 60 \text{ Torr}
 \end{aligned}$$

The numbers beside the data points give the temperature indicated by the centerline thermocouple.



DISTANCE O₂ INLET TO PORT, cm

Fig. 7 [Fe] PROFILE

\bar{T} = 1589 K
 \bar{v} = 48.6 m sec⁻¹
 $[O_2]$ = 0.89×10^{15} ml⁻¹
 λ = 3720 Å
 P = 15 Torr

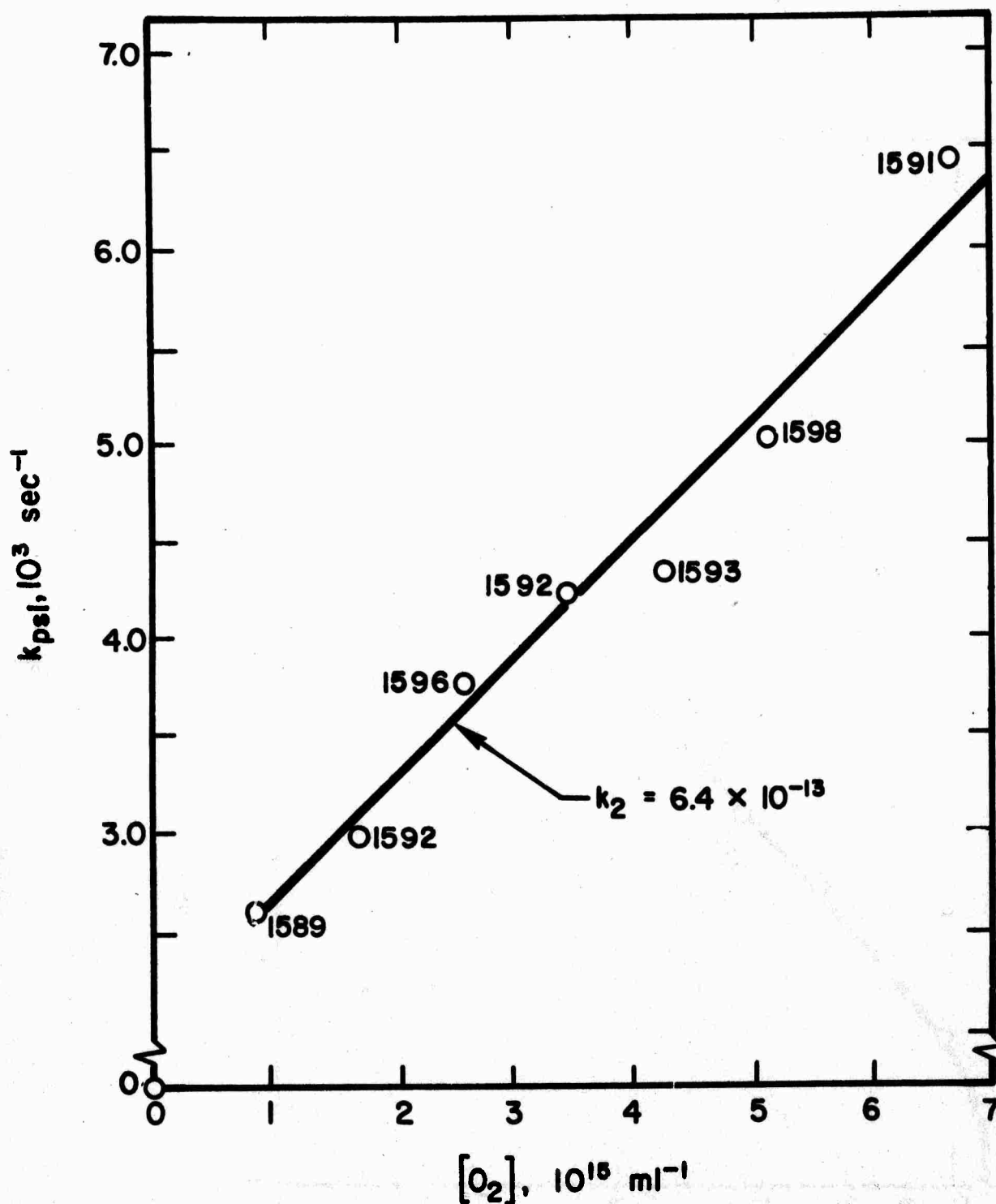
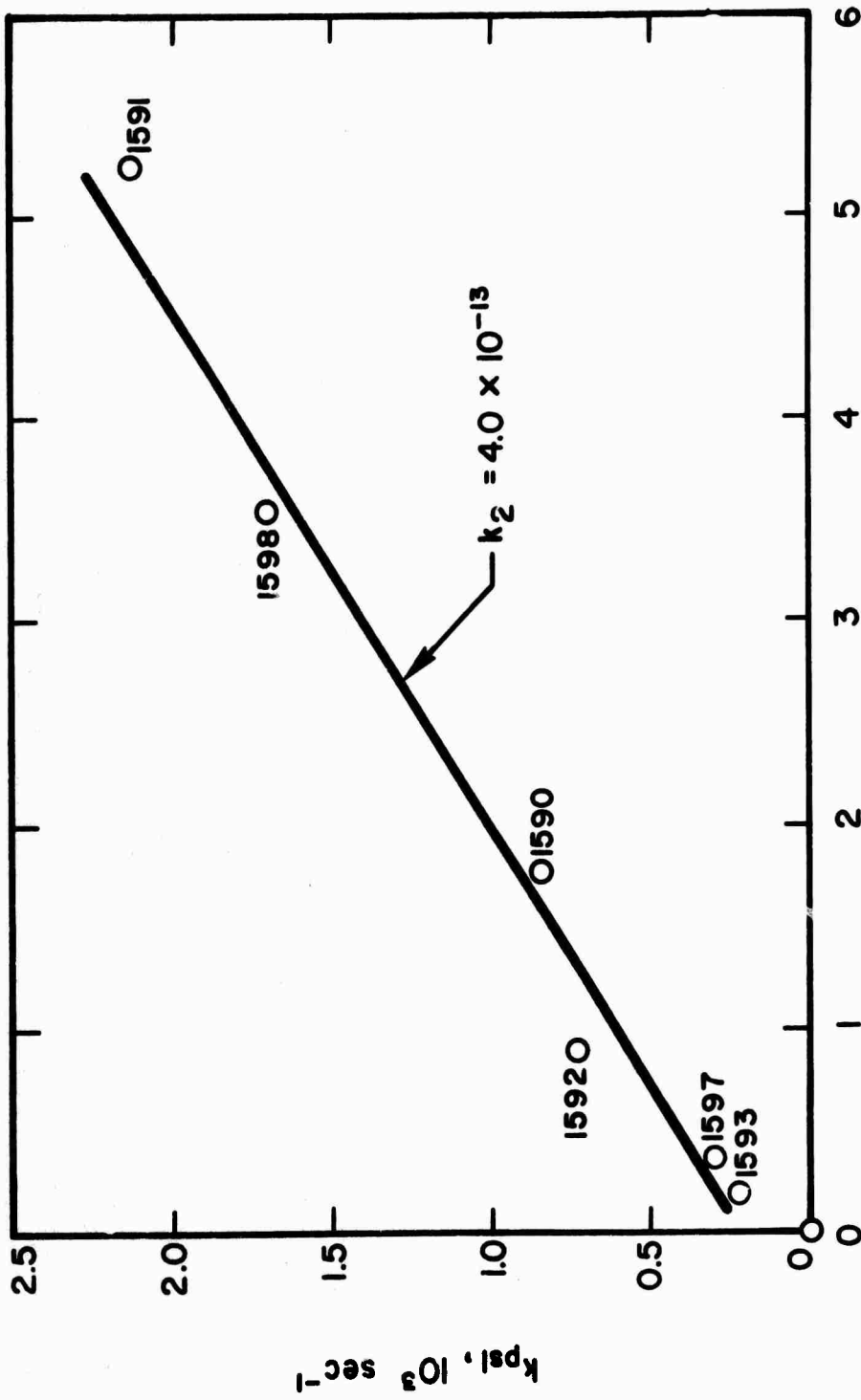


FIG. 8 Fe/O₂ REACTION RATE COEFFICIENT AT 15 TORR

$$\begin{aligned} \bar{T} &= 1593 \text{ K} \\ \bar{v} &= 49 \text{ m sec}^{-1} \\ [M] &= 0.91 \times 10^{17} \text{ ml}^{-1} \\ \lambda &= 3720 \text{ \AA} \end{aligned}$$

Numbers beside each individual data point indicate the \bar{T} at which it was obtained.

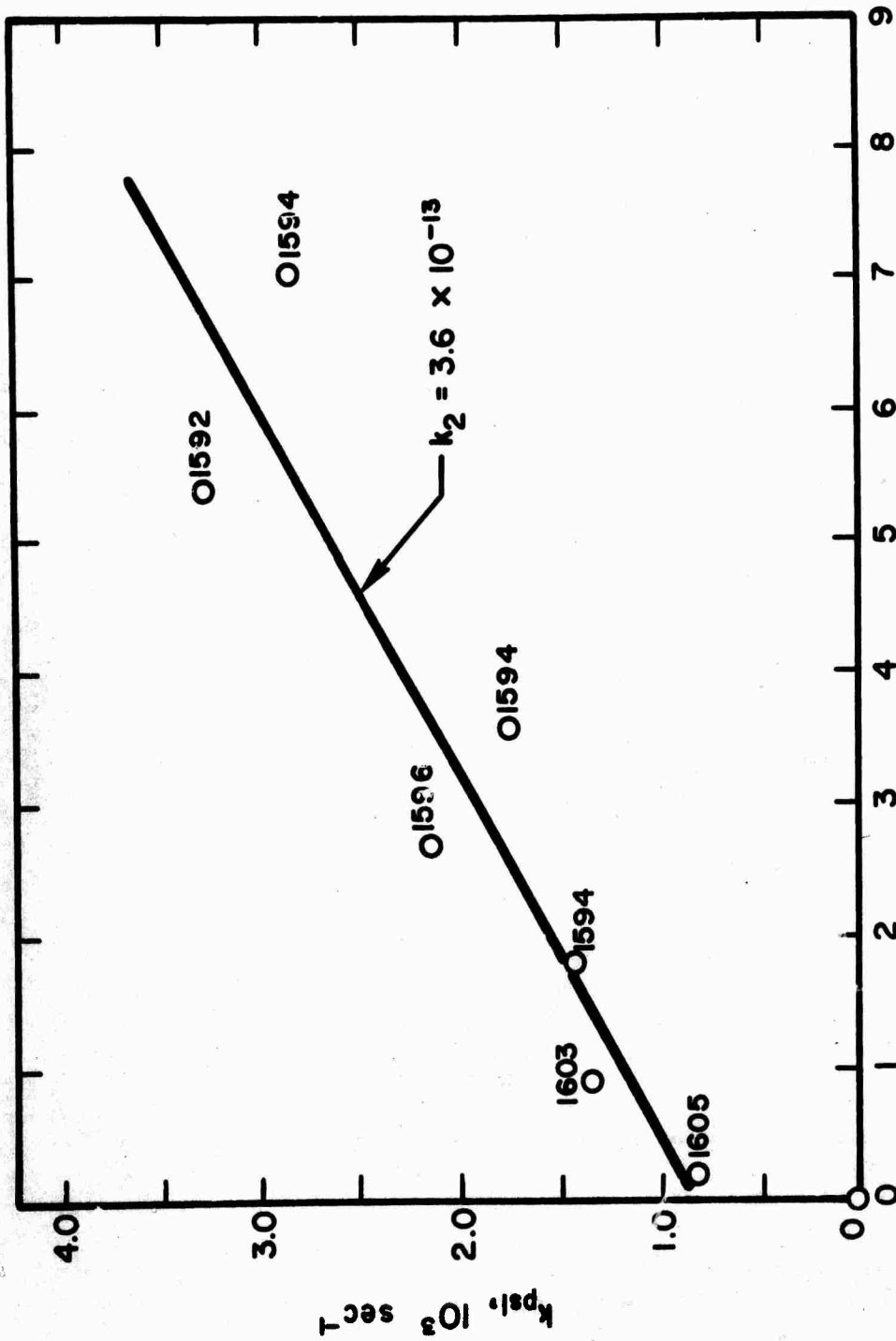


$[\text{O}_2], 10^{15} \text{ ml}^{-1}$

FIG. 9 Fe/O₂ REACTION RATE COEFFICIENT AT 30 TORR

$$\begin{aligned} \bar{T} &= 1594 \text{ K} \\ \bar{v} &= 24 \text{ m sec}^{-1} \\ [\text{M}] &= 1.82 \times 10^{17} \text{ ml}^{-1} \\ \lambda &= 3720 \text{ \AA} \end{aligned}$$

Numbers beside each individual data point indicate the \bar{T} at which it was obtained.



[O₂], 10¹⁵ ml⁻¹

FIG. 10 Fe/O₂ REACTION RATE COEFFICIENT AT 60 TORR

$$\bar{T} = 1597 \text{ K}$$

$$\bar{v} = 24 \text{ m sec}^{-1}$$

$$[M] = 3.64 \times 10^{17} \text{ ml}^{-1}$$

$$\lambda = 3720 \text{ \AA}$$

Numbers beside each individual data point indicate the \bar{T} at which it was obtained.